

Pyruvate secreted from patient-derived cancer-associated fibroblasts supports survival of primary lymphoma cells

Akihiko Sakamoto^{1,2} | Shunsuke Kunou¹ | Kazuyuki Shimada^{1,3}  | Makoto Tsunoda⁴ | Tomohiro Aoki¹ | Chisako Iriyama¹ | Akihiro Tomita¹ | Shigeo Nakamura⁵ | Fumihiko Hayakawa¹ | Hitoshi Kiyoi¹

¹Department of Hematology and Oncology, Nagoya University Graduate School of Medicine, Nagoya, Japan

²Department of Mechanism of Aging, National Center for Geriatrics and Gerontology, Obu, Japan

³Institute for Advanced Research, Nagoya University, Nagoya, Japan

⁴Graduate School of Pharmaceutical Sciences, The University of Tokyo, Tokyo, Japan

⁵Department of Pathology and Clinical Laboratories, Nagoya University Hospital, Nagoya, Japan

Correspondence

Kazuyuki Shimada, Department of Hematology and Oncology, Nagoya University Graduate School of Medicine, Nagoya, Japan.
Email: kshimada@med.nagoya-u.ac.jp

Present address

Chisako Iriyama and Akihiro Tomita, Department of Hematology, Fujita Health University School of Medicine, Toyoake, Japan

Funding information

Ministry of Education, Culture, Sports, Science and Technology; Japan Agency for Medical Research and Development; The Hori Sciences and Arts Foundation; Japan Society for the Promotion of Science; Grant-in-Aid for Scientific Research, Grant/Award Number: 17K08234, 17K09922; Grant-in-Aid for Young Scientists, Grant/Award Number: 26860724

Cancer-associated fibroblasts (CAF) are a key component in the tumor microenvironment and play functional roles in tumor metastasis and resistance to chemotherapies. We have previously reported that CAF isolated from lymphoma samples increase anaerobic glycolysis and decrease intracellular production of reactive oxygen species, promoting the survival of tumor cells. Herein, we analyzed the mechanisms underlying this support of tumor-cell survival by CAF. As direct contact between lymphoma cells and CAF was not indispensable to survival support, we identified that the humoral factor pyruvate was significantly secreted by CAF. Moreover, survival of lymphoma cells was promoted by the presence of pyruvate, and this promotion was canceled by inhibition of monocarboxylate transporters. Metabolome analysis of lymphoma cells in coculture with CAF demonstrated that intermediates in the citric acid cycle were significantly increased, indicating that tumor cells produced energy by aerobic metabolism. These findings indicate that energy production in lymphoma cells is regulated in coordination not only with anaerobic glycolysis, but also with aerobic metabolism termed the reverse-Warburg effect, involving the secretion of pyruvate from CAF resulting in increased use of the citric acid cycle in lymphoma cells.

KEYWORDS

cancer-associated fibroblast, Krebs cycle, lymphoma, pyruvate, reverse Warburg effect

Sakamoto and Kunou contributed equally to this work.

This is an open access article under the terms of the Creative Commons Attribution-NonCommercial-NoDerivs License, which permits use and distribution in any medium, provided the original work is properly cited, the use is non-commercial and no modifications or adaptations are made.

© 2018 The Authors. *Cancer Science* published by John Wiley & Sons Australia, Ltd on behalf of Japanese Cancer Association.

1 | INTRODUCTION

Malignant lymphoma is the most common hematological malignancy. As indicated by the existence of more than 80 subtypes in the current World Health Organization classification, the disease is quite heterogeneous.¹ In terms of B-cell lymphoma, application of anti-CD20 monoclonal antibodies targeting common B-cell antigens has improved clinical outcomes for the disease.²⁻⁴ However, about half of patients with malignant lymphoma show refractory disease, and dealing with intractable cases thus continues to be a priority.

Many recent studies have indicated that genetic abnormalities of *MYC* and *BCL2* in tumor cells are closely associated with the poor prognosis of B-cell lymphoma.⁵⁻⁸ In contrast, as shown by the clinical efficacies of anti-programmed cell death protein 1 (anti-PD1) antibody for Hodgkin lymphoma (HL) and extranodal natural killer (NK)/T-cell lymphoma, the tumor microenvironment (TME) is deeply involved in susceptibility to chemotherapies.⁹⁻¹¹ The TME comprises tumor cells and multiple non-cancerous cells, including fibroblasts, endothelial cells, pericytes, and immunoregulatory cells surrounding neoplastic cells.¹² Interactions between tumor cells and non-cancerous cells develop a favorable microenvironment for tumor cells, resulting in the acquisition of resistance to various therapies.¹³

Fibroblasts are known to represent one of the key components of tumor stroma, and many studies have suggested a prominent functional role for cancer progression and metastasis.^{12,14} Fibroblasts associated with cancer are activated and have been termed cancer-associated fibroblasts (CAF). In the TME of various tumors, humoral factors released from CAF play fundamental roles in tumor metastasis, resistance to chemotherapy, and epithelial-to-mesenchymal transition (EMT).¹⁵⁻²⁰ In malignant lymphoma, we have previously reported that a mouse-derived fibroblastic reticular cell (FRC) line supported lymphoma cells from patient-derived xenograft (PDX) models, indicating that fibroblasts also play many functional roles in the lymphoma microenvironment.^{21,22} This report examined how CAF isolated from primary lymphoma samples support primary lymphoma cells in vitro and clarified the components vital for these abilities.

2 | MATERIALS AND METHODS

2.1 | Patient samples

Samples from patients who received lymph node biopsies were obtained at Nagoya University Hospital. The study protocol for the experimental use of patient samples was approved by the institutional review board of Nagoya University Hospital and complied with all provisions of the Declaration of Helsinki and the Ethics Guidelines for Human Genome/Gene Analysis Research issued by the Ministry of Health, Labour and Welfare in Japan. All lymph node samples for banking and analyses were obtained from patients with lymphoid malignancies, after obtaining written informed consent.

2.2 | Establishment of patient-derived CAF

Patient-derived CAF were established as described previously.²² In brief, residue from a fresh patient sample mashed to obtain a cell suspension for diagnostic analyses was loosened in 0.25% trypsin-EDTA solution, then placed into a 10-cm dish with Iscove's modified Dulbecco's medium (Sigma-Aldrich, St Louis, MO, USA) supplemented with 10% FBS (Gibco in Thermo Fisher Scientific, Waltham, MA, USA) and 2 mmol/L glutamine (Gibco). Of the various types of cells in this culture, only those spindle-shaped adherent cells with α -smooth muscle actin (SMA)-positive, CD31-negative results survived for more than several months. As such adherent cells were not established from benign disease samples, the adherent cells were regarded as CAF. CAF were maintained in RPMI 1640 Medium (Sigma-Aldrich) supplemented with FBS and glutamine as mentioned above by splitting them once a week.

2.3 | Expansion of primary tumor samples

Primary tumor samples were expanded as follows. Fresh patient samples were mashed and filtered through 70- μ m culture mesh, followed by coculture with the established CAF in the above-mentioned RPMI culture medium. Whole non-adherent samples were serially cocultured with the CAF split once a week. After about 1 month, subsets of non-adherent cells were expanded, which were confirmed as B-cell lymphoma cells by flow cytometry. The expanded tumor cells were maintained by coculture with CAF, and experiments using the expanded tumor cells were carried out within 1 month.

2.4 | Isolation of tumor cells

Primary B-cell lymphoma cells or reactive B-cell counterparts were magnetically isolated from frozen samples using CD19 beads (Miltenyi Biotec, Bergisch Gladbach, Germany).

2.5 | RNA preparation and RT-PCR

To evaluate expressions of monocarboxylate transporter (MCT) genes including *MCT1*, *MCT2*, *MCT3*, *MCT4*, *SMCT1*, and *SMCT2*, and *GAPDH* as an internal control, total RNA from patient cells was extracted using QIAamp RNA Blood Mini Kit (QIAGEN, Venlo, the Netherlands), then cDNA was prepared using SuperScript II Reverse Transcriptase (Invitrogen in Thermo Fisher Scientific) according to the manufacturer's protocol. To detect the above genes, the primers listed in Table S1 were used. Messenger RNA fragments of *MCT1*, *MCT2*, *MCT3*, *MCT4*, *SMCT1*, *SMCT2* and *GAPDH* were amplified with GoTaq Green (Promega, Madison, MI, USA) using an ABI 3500 genetic analyzer (Applied Biosystems in Thermo Fisher Scientific).

2.6 | Immunoblotting

Immunoblotting was carried out using the following antibodies appropriately diluted in TBS-Tween buffer containing 5% BSA and 0.05% sodium azide: anti-cleaved caspase 3 (CC3) (clone 5A1E;

Cell Signaling Technology, Danvers, MA, USA), anti- γ H2A.X (S139) (GTX127340; GeneTex, Irvine, CA, USA), and anti-GAPDH (sc-25778; Santa Cruz Biotechnology, Dallas, TX, USA). The experimental procedures have been described previously.²³ Images were obtained using a LAS4000mini bio-imager (FUJIFILM, Tokyo, Japan) and analyzed using MultiGauge software (FUJIFILM).

2.7 | Cell death assessment

To evaluate cell death for monocultured tumor cells, propidium iodide (PI) and annexin V-FITC assay were carried out as detailed previously.^{23,24} In brief, cells were placed in 96-well plates and incubated with the required drugs or pyruvate for the appropriate time, then stained with 10 μ g/mL PI and 10 μ g/mL annexin V-FITC for 15 minutes at 4°C in the dark. Cell death was assessed by flow cytometry (FACSCalibur; Becton, Dickinson and Co. (BD), Franklin Lakes, NJ, USA) and analyzed using FlowJo version 10.3 software (TreeStar, Ashland, OR, USA).

2.8 | Surface antigens and intracellular antigen analysis

Surface staining was carried out at 4°C using the following antibodies: anti-intercellular adhesion molecule 1 (ICAM1) (clone 15.2; Bio-Rad Laboratories, Hercules, CA, USA), anti-vascular cell adhesion protein 1 (VCAM1) (clone 1.G11B1; Bio-Rad Laboratories), anti-CD44 (clone IM7; BioLegend, San Diego, CA), anti-CD45 (clone HI30; BD), anti-CD31 (clone MEM-05; EXBIO, Vestec, Czech Republic), anti-CD21 (clone Bu32; BioLegend), and anti-CD35 (clone E11; BioLegend). For intracellular staining, samples were fixed in 4% paraformaldehyde, followed by permeabilization in 0.1% Triton X-100. Samples were then intracellularly stained with anti- α SMA (clone 1A4; R&D Systems, Minneapolis, MN, USA) at 4°C. Antigens were assessed by flow cytometry as described above.

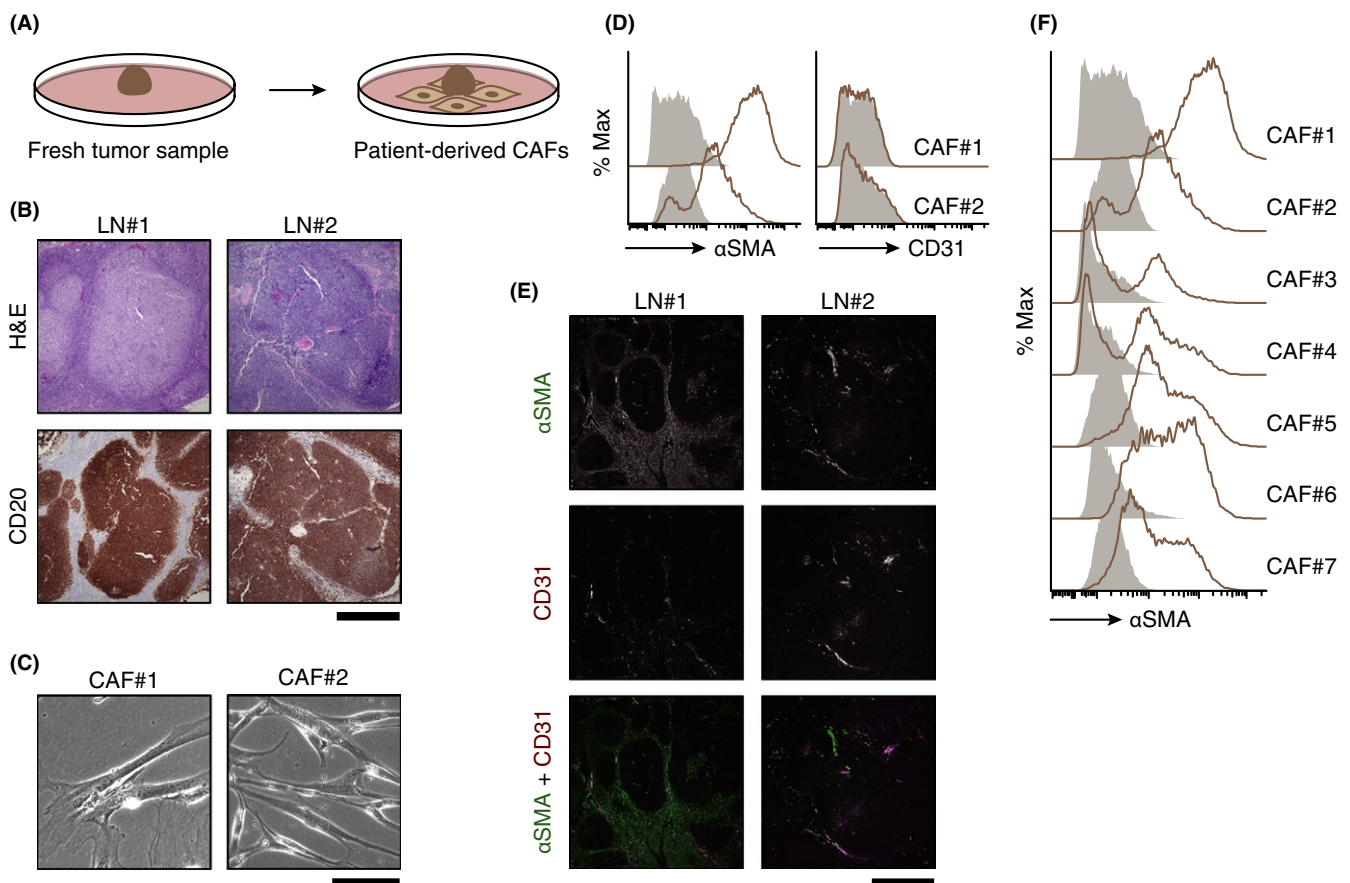
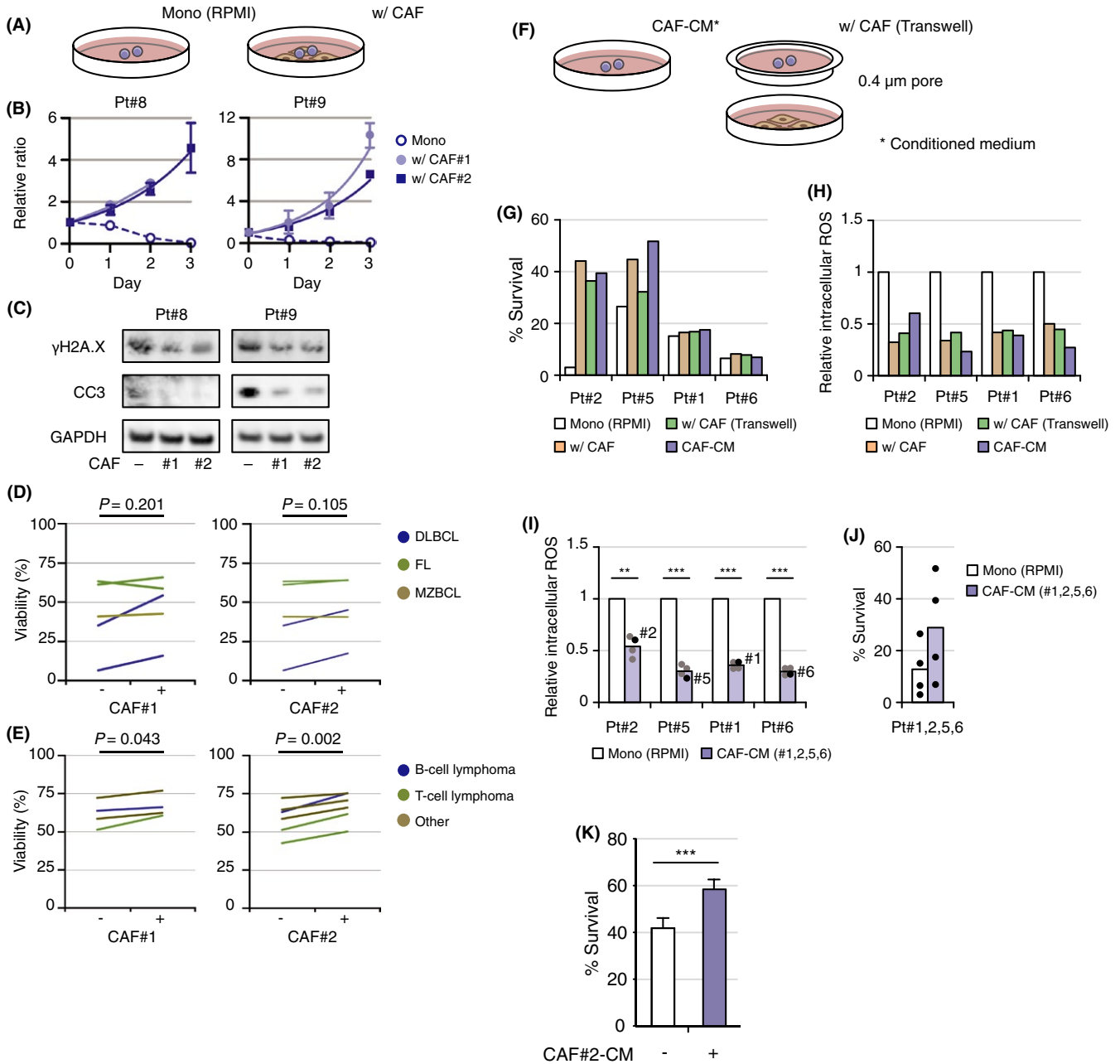


FIGURE 1 Establishment of cancer-associated fibroblasts (CAF) from primary patient lymph node samples. A, Scheme for establishment of primary lymph node samples. B, Pathological specimens of lymph node samples (LN#1 and LN#2) are shown. H&E and CD20 staining of LN#1 (upper left and lower left columns) and LN#2 (upper right and lower right columns) are shown. Representative CAF#1 and CAF#2 originated from these lymph node samples, respectively. Scale bar, 1 mm. C, Phase-contrast images of representative CAF#1 (left) and CAF#2 (right) are shown. Scale bar, 100 μ m. D, Expression of surface antigens of CAF evaluated on flow cytometry (FCM). Expression of surface antigens was analyzed using anti- α smooth muscle actin (anti- α SMA) (left) and anti-CD31 (right) antibodies. Isotype-matched controls are shown as filled histograms. E, Immunofluorescence staining of pathological specimens of LN#1 and LN#2. Specimens were analyzed using anti- α SMA (green) and anti-CD31 (red) antibodies; anti- α SMA (upper left and upper right), anti-CD31 (middle left and middle right), and merged (lower left and lower right). Scale bar, 1 mm. F, Expression of α SMA of established CAF. Established CAF (CAF#1 to CAF#7) were evaluated on FCM using anti- α SMA



2.9 | Immunohistochemistry

Formalin-fixed, paraffin-embedded tissues of patient samples were evaluated by routine H&E staining and immunohistochemistry using the following primary antibodies: anti-CD20 (clone L26; Dako, Glostrup, Denmark), anti- α SMA (Dako), and anti-CD31 (ab28364; Abcam, Cambridge, UK). The staining procedure for immunohistochemistry was as described previously.²⁴ Specimens were observed using a BX51 N-34 microscope (Olympus, Tokyo, Japan), and the photographs were taken with a BZ9000 (Keyence, Osaka, Japan).

2.10 | Evaluation of intracellular reactive oxygen species

Levels of intracellular reactive oxygen species (ROS) were measured using 2',7'-dichlorofluorescein diacetate (Cayman Chemical, Ann Arbor, MI, USA). After incubation of cells with 1 mmol/L 2',7'-dichlorofluorescein diacetate for 30 minutes at 37°C, the supernatant was removed and the cells were incubated with complete media for 1 hour at 37°C. Fluorescence was then measured on the GloMax-Multi+ Detection System (Promega Biosystems Sunnyvale, Sunnyvale, CA, USA).

FIGURE 2 Cancer-associated fibroblasts (CAF) and conditioned media support survival of primary lymphoma cells. A, Scheme of coculture of primary lymphoma cells with CAF. B, Proliferation of primary lymphoma cells (Pt#8, left; Pt#9, right) in monoculture (open circle) and coculture with CAF#1 (circle) and CAF#2 (square). Survival of tumor cells was evaluated by Trypan blue exclusion. Each point represents the mean value taken from three independent experiments with error bars indicating the standard error of the mean. C, Immunoblotting for γ H2A.X, CC3, and GAPDH as a loading control in Pt#8 and Pt#9 in monoculture and coculture with CAF#1 and CAF#2 was carried out. D, Viability of three histological types of primary B-cell lymphoma cells (DLBCL, indigo blue; FL, green; MZBCL, brown) in coculture with CAF#1 (left) and CAF#2 (right) overnight are shown. Each point represents the mean value of two technical replicates taken from a single experiment. E, Viability of a different lineage of lymph node samples including B-cell lymphoma (indigo blue), T-cell lymphoma (green) and others such as related disease or reactive tissue (brown) in coculture with CAF#1 and CAF#2 overnight are shown. Each point represents the mean value of two technical replicates taken from a single experiment. F, Scheme of culture in the presence of conditioned medium (CM) released from CAF (left), in the absence of direct contact of primary lymphoma cells to CAF by Transwell (upper right), and coculture with CAF (lower right). G, Comparison of survival of primary B-cell lymphoma cells (Pt#2, Pt#5, Pt#1, and Pt#6) in monoculture (white), coculture with CAF (orange), in the absence of direct contact with CAF using the Transwell (green), and in culture with CM released from CAF (blue) overnight are shown. CAF originated from samples corresponding to the examined lymphoma cells. Each bar represents averaged data (two technical replicates) taken from a single experiment. H, Comparisons of redox regulation in B-cell lymphoma cells (Pt#2, Pt#5, Pt#1, and Pt#6) in monoculture (white), coculture with CAF (orange), in the absence of direct contact with CAF using Transwell (green), and in culture with CM released from CAF (blue) are shown. Levels of intracellular ROS were measured using a fluorescent indicator, 2',7'-dichlorofluorescein diacetate. I, Comparisons of redox regulation in B-cell lymphoma cells (Pt#2, Pt#5, Pt#1, and Pt#6) in monoculture, and cultures with CM released from CAF#2, CAF#5, CAF#1, and CAF#6. Blue bars represent mean values for the four conditions. Values of the matched pairs of lymphoma cells and established CAF are indicated as black points, and those of unmatched pairs are indicated as grey points. * $P < .05$, ** $P < .01$, *** $P < .001$. J, Survival of primary B-cell lymphoma cells (Pt#2, Pt#5, Pt#1, and Pt#6) in culture with CM released from the corresponding CAF. Blue bar represents the mean value of the four conditions (Pt#2, Pt#5, Pt#1, and Pt#6) indicated by black points. K, Survival of primary lymphoma cells (Pt#9) in the presence of 100 nmol/L doxorubicin in culture with or without CM released from CAF#2. Cells were treated with doxorubicin for 72 h, before analysis of cell death on flow cytometry. Each bar represents averaged data (two technical replicates) taken from five independent experiments. Error bars indicate SD

2.11 | Evaluation of metabolic activities

Metabolic activities were measured using calcein acetoxymethyl ester. After incubation of cells with 1 μ mol/L calcein acetoxymethyl ester for 30 minutes at 37°C, fluorescence was measured on the GloMax-Multi+ Detection System (Promega). Concentrations of intracellular pyruvate or pyruvate in the medium were measured using a Pyruvate Colorimetric/Fluorometric assay kit (BioVision, Milpitas, CA, USA) in accordance with the protocol from the manufacturer. Absorbance was measured on the GloMax-Multi+ Detection System (Promega). To inhibit MCT, α -cyano-4-hydroxycinnamic acid (4-CIN) (Sigma-Aldrich) was used. Cells were incubated with 500 μ mol/L 4-CIN for 12 hours at 37°C, then cells were evaluated by appropriate procedures for each assay.

2.12 | Metabolome analysis

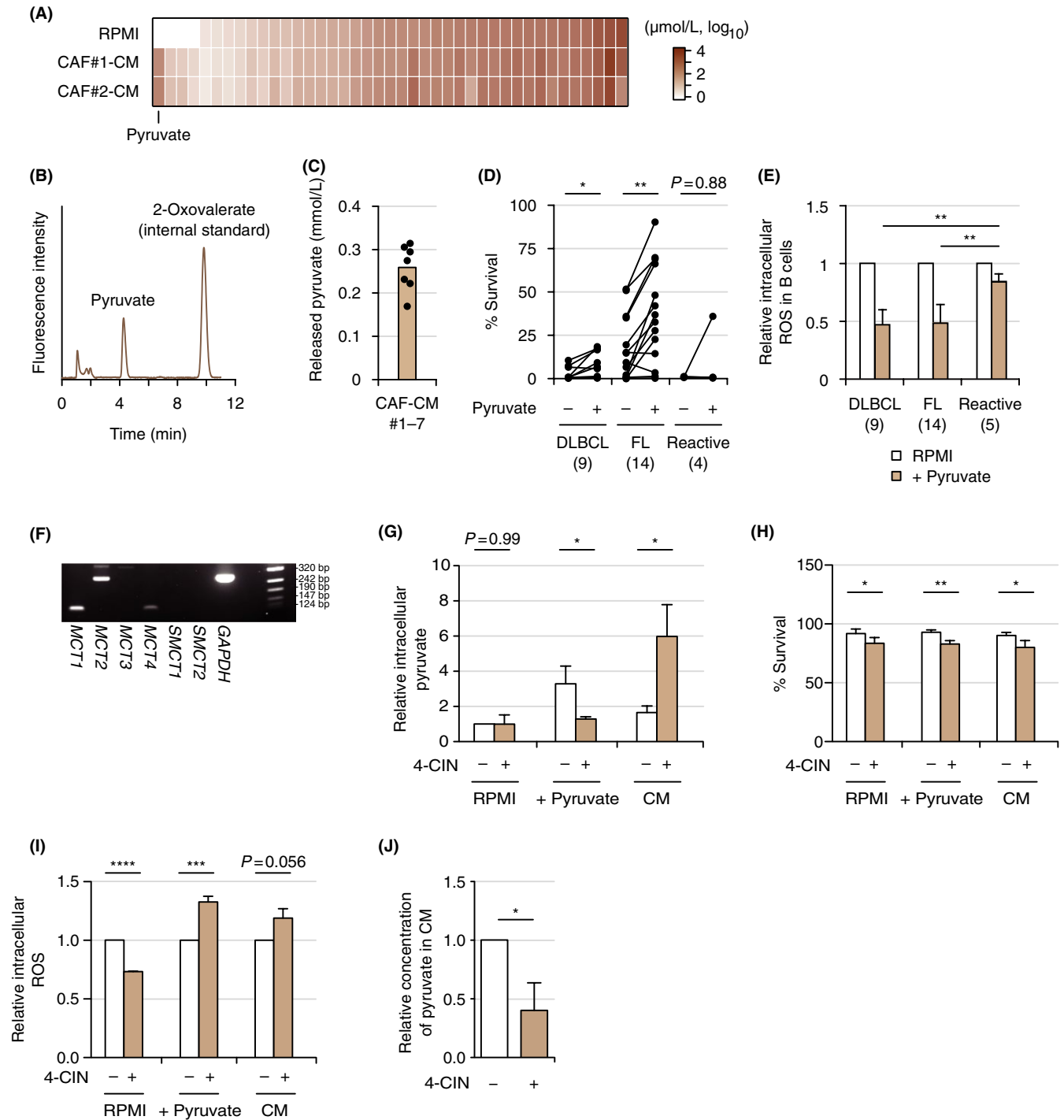
To analyze comprehensive metabolites secreted from CAF, metabolomic analyses were carried out. In brief, intracellular metabolites were extracted with methanol. Culture supernatants or cell extracts were dried in vacuum and re-solubilized in Milli-Q water (Merck Millipore, Billerica, MA, USA) for capillary electrophoresis-time-of-flight mass spectrometry (CE-TOFMS) analysis. Metabolite analysis using a CE-TOFMS system²⁵ was carried out by Human Metabolome Technologies (Tsuruoka, Japan). Concentrations of metabolites were determined from corresponding peak areas normalized to those of the internal standard (H3304-1002; Human Metabolome Technologies) using three-point calibration curves.

2.13 | High-performance liquid chromatography analysis

To determine the quantities of specific metabolites in supernatants of CAF, HPLC analyses were also carried out. Supernatants of CAF cultures were mixed with the internal standard 2-oxovalerate and reacted with 10 mmol/L *o*-phenylenediamine in 2-mol/L HCl for 20 minutes at 80°C. Samples were desiccated with sodium sulfate, dried in vacuum, and re-solubilized in methanol for HPLC analysis. Fluorescent derivatives were separated on an HPLC system comprising a pump (PU-1580; JASCO, Tokyo, Japan), an auto sampler (AS920; JASCO), a column oven (CO980; JASCO), and a fluorescence detector (FP1520; JASCO). HPLC was carried out on an octadecylsilica column (Inertsil ODS-4, 250 \times 3.0 mm internal diameter, 5 μ m; GL Sciences, Tokyo, Japan) at 40°C with a flow rate of 0.6 mL/min, using a mobile phase comprising water/methanol (55/45, v/v).

2.14 | Statistical analysis

Quantitative results using available cell lines or primary lymphoma cells are presented as mean \pm standard error of the mean or SD taken from two or three independent experiments. When repeated experiments were difficult using limited primary samples, data were taken from a single experiment. The statistical significance of in vitro experiments was evaluated using an unpaired *t*-test or by two-way analysis of variance, with values of $P < .05$ considered significant. All statistical analyses were done using R software (R Foundation for Statistical Computing, Vienna, Austria) or GraphPad PRISMv7 (GraphPad Software Inc., La Jolla, CA, USA).



3 | RESULTS

3.1 | Isolation of CAF from primary patient samples with lymphoid malignancies

At least in part of primary patients' samples, adherent cells could be initiated to proliferate on the bottom of the dish (Figure 1A). Representative pathological specimens for which adherent cells were able to be cultured at an early stage in our study are shown in Figure 1B. For lymph nodes (LN) of two patients (Pt)#1 and Pt#2,

the structure of lymphoid follicles was retained and outgrowth of CD20-positive tumor cells was seen to lead to the diagnosis of follicular lymphoma (Figure 1B; Table S2). Continued culture of adherent cells proliferating on the bottom of the dish allowed successful isolation of fibroblasts (Figure 1C). Isolated fibroblasts could be cultured for a long time, and flow cytometric analysis showed that those fibroblasts were positive for αSMA , activated myoblast markers, and negative for CD31, vascular endothelial markers, indicating that the characteristics of these fibroblasts coincided with those of CAF (Figure 1D).¹² Other surface phenotypes of those fibroblasts

FIGURE 3 Pyruvate as the fundamental metabolite in cancer-associated fibroblasts (CAF). A, Comparison of metabolites between RPMI and conditioned medium (CM) released from CAF#1 and CAF#2 evaluated by capillary electrophoresis-time-of-flight mass spectrometry (CE-TOFMS). Data are sorted by concentrations of metabolites in RPMI. B, Confirmation of release of pyruvate from CAF by HPLC. C, Concentrations of pyruvate released in CM from CAF. Brown bar indicates the mean value of conditioned mediums from CAF#1 to CAF#7 measured by HPLC. Each point (black) represents the concentration of pyruvate in CM released from each CAF, as the mean of data from three experiments. D, Comparison of viabilities of primary lymphoma cells (diffuse large B-cell lymphoma [DLBCL], $n = 9$; follicular lymphoma [FL], $n = 14$; and reactive tissues, $n = 4$) in the presence or absence of 0.25 mmol/L pyruvate is shown. Viability was evaluated by the propidium iodide (PI)-Annexin V method on flow cytometry (FCM). Corresponding samples in the presence or absence of pyruvate are connected with a straight line. Each point represents the mean of two individual technical replicates taken from a single experiment. $*P < .05$, $**P < .01$, $***P < .001$, $****P < .0001$. E, Comparison of redox regulation in primary lymphoma cells (DLBCL, $n = 9$; FL, $n = 14$; reactive tissues, $n = 5$) in the presence or absence of 0.25 mmol/L pyruvate. Each bar indicates the mean value of primary lymphoma samples indicated taken from a single experiment (two technical replicates) with error bar indicating SD. F, RT-PCR analysis of monocarboxylate transporter (MCT; *MCT1*, *MCT2*, *MCT3*, *MCT4*, *SMCT1*, and *SMCT2*) in Pt#9 cells. PCR using primers for GAPDH was carried out as an internal control. G-I, Significance of the inhibition of MCT by α -cyano-4-hydroxycinnamic acid (4-CIN) in Pt#9 cells in culture with RPMI, RPMI on addition of pyruvate, and CM. Relative intracellular pyruvate (G), survival analysis on FCM (H), and relative intracellular ROS (I) are shown. Each bar indicates the mean from three or four independent experiments (two technical replicates) with error bar indicating SD. J, Relative concentration of pyruvate in CM released from CAF#2 in the presence or absence of 4-CIN. Each bar indicates the mean taken from four independent experiments (two technical replicates) with error bar indicating SD

were negativity for CD45, CD21, CD35, and VCAM1, and positivity for ICAM1 and CD44 (Figure S1). Fluorescent immunohistochemical staining for pathological specimens showed that α SMA-positive fibroblasts and CD31-positive blood vessels existed around neoplastic follicles (Figure 1E). To expand our considerations, we continued to culture other lymphoma samples. Fibroblasts were isolated from seven patients with lymphoma (Table S2). All cells showing positive results for α SMA were considered to represent CAF (Figure 1F). CAF that were culturable for more than 2-3 months were isolated from neoplastic lymph nodes only, not from reactive tissue (data not shown).

3.2 | Support of tumor cell survival by CAF

We have previously reported that the BLS4 mouse FRC line, which was established from a mouse lymph node,²⁶ enabled culture of

PDX lymphoma cells²¹ and that CAF also supported survival of primary patient lymphoma cells in vitro.²² Primary patient lymphoma cells (Pt#8 with Burkitt lymphoma, and Pt#9 with high-grade B-cell lymphoma, not otherwise specified) could proliferate in coculture with CAF#1 and CAF#2 in vitro, whereas neither cell type could survive in monoculture (Figure 2A,B; Table S2). For immunoblotting to evaluate cell death, higher expression of γ H2A.X and cleaved caspase 3 resulting from DNA double-strand breaks in lymphoma cells leading to apoptosis were detected in monoculture (Figure 2C). We next expanded the analysis to determine whether three different types of primary B-cell lymphoma cells from lymph node biopsies could survive in coculture with CAF. Survival of primary lymphoma cells in coculture with CAF differed among histological subtypes; survival support was observed in both of two primary diffuse large B-cell lymphoma (DLBCL) cells and in one of two primary follicular lymphoma (FL) cells. The remaining primary lymphoma cells from a

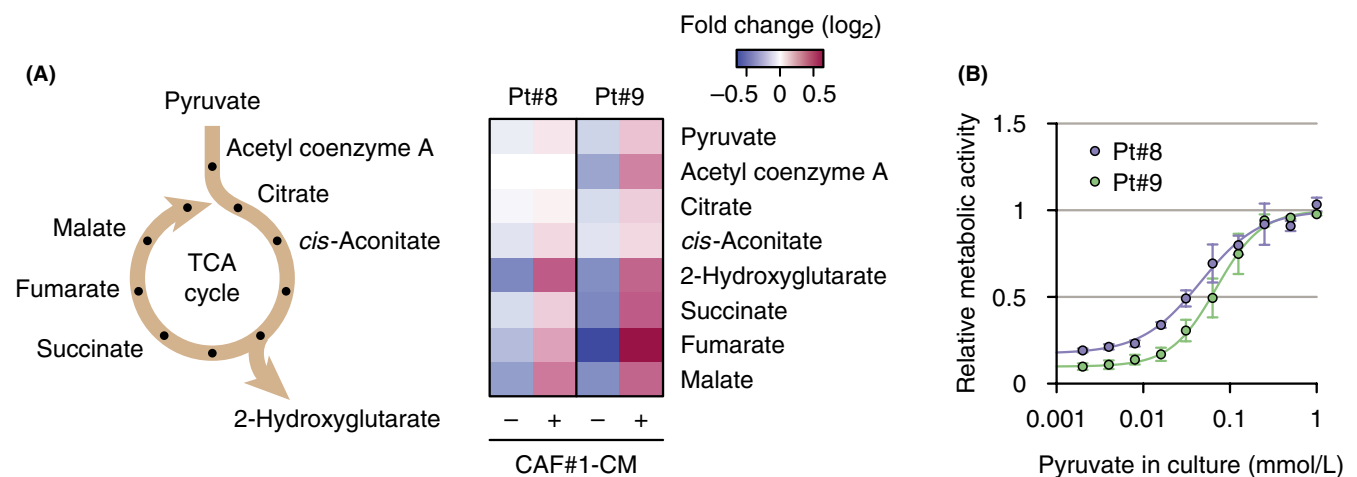


FIGURE 4 Increased citric acid cycle in primary lymphoma cells in culture with conditioned medium (CM). A, Scheme of citric acid cycle (left) and increased intermediates in the cycle in lymphoma cells under culture with CM released from CAF#1 (right). Intermediates were measured by capillary electrophoresis-time-of-flight mass spectrometry. B, Relative metabolic activities in Pt#8 and Pt#9 cultured overnight in RPMI medium supplemented with the indicated concentrations of pyruvate are shown. Values were measured using a fluorescent indicator calcein.²⁷ Each point represents the mean value taken from three independent experiments, with error bars indicating SEM. CAF, cancer-associated fibroblast

patient with marginal zone B-cell lymphoma (MZBCL) were not supported (Figure 2D; Table S2). In addition, we analyzed whether survival support from CAF differed among lineages of lymphoma cells. Intriguingly, primary lymphoma cells could survive irrespective of lineage, including B cells and T cells (Figure 2E; Table S2). We thus hypothesized that some types of humoral factors from CAF were associated with such support of survival for primary lymphoma cells. Survival support of primary B-cell lymphoma cells (Pt#1, Pt#2, Pt#5, and Pt#6; numbers indicating each patient match with corresponding CAF in Table S2) was analyzed in culture with conditioned medium with CAF or in the absence of direct contact between CAF and lymphoma cells using separation by a Transwell with a pore size of 0.4 μm (Figure 2F). As expected, survival support from CAF was observed not only in the presence of direct contact between tumor cells and CAF, but also in the absence of direct contact and under coculture in conditioned medium with CAF (Figure 2G). In terms of redox regulation, intracellular ROS uniformly decreased in the presence of direct or indirect contact between CAF and lymphoma cells (Figure 2H). The extent of survival support in patient lymphoma cells varied according to the type of support from CAF. Analyzed from the perspective of conditioned medium released from matched or unmatched CAF with the corresponding patient lymphoma cells, we could not detect apparent differences in ROS production (Figure 2I). Survival of lymphoma cells cultured with conditioned medium released from CAF from the corresponding patient varied, but was higher than survival with normal complete media (Figure 2J). In addition, the increased survival of lymphoma cells cultured with conditioned medium contributed to resistance to the anticancer drug doxorubicin (Figure 2K). Collectively, these data indicate that humoral factors from CAF could be involved in survival support of patient lymphoma cells.

3.3 | Role of pyruvate released from CAF in survival support

We next analyzed the metabolites from CAF that contribute to survival support. Among 41 metabolites analyzed using CE-TOFMS assay, pyruvate was identified as the most increased metabolite secreted into the conditioned medium from CAF (Figure 3A; Table S3). We also confirmed that pyruvate was secreted into the media at higher concentrations in HPLC (Figure 3B,C). Addition of pyruvate to culture media contributed significantly to survival of primary DLBCL ($n = 9$) and FL cells ($n = 14$) (Figure 3D). In line with the increased survival seen on addition of pyruvate to culture media, intracellular ROS production was decreased in DLBCL and FL cells (Figure 3E). We subsequently evaluated the significance of pyruvate released from CAF for primary lymphoma cells by the inhibition of MCT involved in the uptake and efflux of pyruvate. Expression of MCT of tumor cells was initially confirmed (Figure 3F). In the presence of complete media supplemented with pyruvate, the MCT inhibitor 4-CIN decreased the concentration of intracellular pyruvate, probably through inhibition of pyruvate uptake from culture media (Figure 3G). Addition of 4-CIN to both complete media with

pyruvate and conditioned medium from CAF decreased cell survival and increased ROS production (Figure 3H,I). Moreover, the concentration of pyruvate in the conditioned medium from CAF decreased in the presence of 4-CIN (Figure 3J). Together, these data indicate that pyruvate secreted from CAF at high concentration decreased intracellular ROS production by primary lymphoma cells, resulting in survival of these cells. Furthermore, this secretion and the resulting effects were, at least in part, canceled by the inhibition of MCT.

3.4 | Culture with conditioned medium increases the citric acid cycle in tumor cells

Finally, we analyzed the types of metabolites in patient tumor cells that were modulated by culture with conditioned medium. In the presence of conditioned medium from CAF#1, intermediates in the citric acid cycle including 2-hydroxyglutarate, succinate, fumarate, and malate increased in patient tumor cells (Pt#8 and Pt#9) (Figure 4A). Metabolic activity in tumor cells was increased in a pyruvate dose-dependent way (Figure 4B). These data indicate that pyruvate secreted from CAF increased the citric acid cycle in tumor cells, leading to cell survival.

4 | DISCUSSION

In this analysis, we successfully isolated CAF from primary lymph node samples in patients with malignant lymphoma. CAF significantly secreted pyruvate, which might have been taken up by neighboring tumor cells, increasing the citric acid cycle, and leading to decreased redox regulation and survival of tumor cells. Anaerobic glycolysis is generally increased in tumor cells, representing the Warburg effect.²⁸ A previous report showed that epithelial cancer cells induced aerobic glycolysis in stromal fibroblasts, then underwent myofibroblastic differentiation to secrete lactate and pyruvate. Tumor cells then showed uptake of energy-rich metabolites and used them in the citric acid cycle, recognized as the reverse Warburg effect.²⁹ Our findings might support this effect existing not only in epithelial tumor cells, but also in lymphoma cells.

In the present study, we were able to isolate CAF from various types of lymphoid malignancies, including DLBCL, FL, and HL. Considering that long-term culture of fibroblasts from reactive lymph nodes was considered impossible, fibroblasts are widely activated as CAF in malignant lymphoid tumors irrespective of the histological type. However, we observed differences in survival support between histological types. We used CAF#1 and CAF#2, which showed strong support of tumor cell survival in this analysis. DLBCL cells tended to be supported by CAF, whereas survival support was not apparent for FL and MZBCL cells. As the difference in survival support between lineages of tumor cells was unclear, the nature of tumor cells in terms of the rate of cell proliferation may be associated with survival support.

In this analysis, the value of survival support by CAF differed between primary lymphoma cells. However, the support of tumor

cell survival did not differ according to the presence or absence of direct contact of tumor cells to stromal cells; that is, survival did not differ significantly among cocultures, cocultures in Transwells, and cultures with conditioned medium from CAF. Moreover, redox regulation in tumor cells did not differ according to the presence of conditioned medium from different CAF (Figure 2I). These findings suggest that humoral factors released from CAF might be critical for support of tumor cell survival. The mechanisms underlying the differences between primary lymphoma cells and the nature of CAF from lymph node samples should be further investigated.

Metabolome analysis showed that pyruvate secreted from CAF plays an important role in supporting tumor cells. Intriguingly, the extent of support of DLBCL cell survival in cocultures with CAF was superior to that of FL cell survival, whereas the extent of FL cell survival support in culture with medium supplemented with pyruvate or conditioned medium from CAF was superior to that of DLBCL cell survival. This discrepancy might be as a result of differences in the nature of tumor cells such as proliferation and dependency on TME. In addition, inhibition of uptake/efflux of pyruvate by the MCT inhibitor 4-CIN decreased survival or increased intracellular ROS production by lymphoma cells. In contrast, the concentration of intracellular pyruvate in lymphoma cells increased in the presence of conditioned medium from CAF with 4-CIN. This paradoxical phenomenon might be a consequence of the inhibition of efflux of intracellular pyruvate. This discrepancy should be further investigated.

In the present analysis, reliance on the citric acid cycle in tumor cells increased in cultures with conditioned medium from CAF. Generally, the TME is known to be under hypoxic conditions and promotes a metabolic switch in tumor cells away from mitochondrial respiration to glycolysis.²⁸ According to our previous report, tumor cells in coculture with CAF promote anaerobic glycolysis as indicated by the increased expressions of HK2 and PDK1.²² Considering the complexity in terms of energy production in tumor cells, tumor cells might coordinate the regulation of aerobic glycolysis and the citric acid cycle according to the specific TME.^{30–32} Clarification of associations between metabolic changes and survival of lymphoma cells represents an interesting topic for future analyses.

In conclusion, we successfully isolated CAF from primary lymph node samples from patients with different types of lymphoma. Pyruvate secreted from CAF appears to play an important role in the survival of tumor cells. Considering that CAF carry out various functions in the TME, the findings of this study could represent only a fraction of what occurs in the TME. Future investigations to uncover the role of CAF in the lymphoma microenvironment may provide a gateway to overcoming this intractable disease.

ACKNOWLEDGMENTS

We would like to thank Mr. Kuniyoshi Kitou, Ms. Kazuko Matsuba, Ms. Yuko Katayama, and Mr. Yoshiaki Inagaki (Nagoya University) for IHC work; Ms. Yoko Matsuyama, Ms. Chika Wakamatsu, Ms. Manami Kira, Ms. Rie Kojima, Ms. Yukie Konishi, Ms. Yuko Kojima, and Ms.

Saori Kanamori (Nagoya University) for assistance with laboratory work. This work was supported by the Program to Disseminate Tenure Tracking System, MEXT, Japan, by a JSPS Grant-in-Aid for Young Scientists (B) 26860724 and Grant-in-Aid for Scientific Research (C) 17K09922, by the Practical Research for Innovative Cancer Control, MHLW/AMED, Japan, and by The Hori Sciences and Arts Foundation grant to K.S., and by a JSPS Grant-in-Aid for Scientific Research (C) 17K08234 grant to M.T.

CONFLICTS OF INTEREST

H.K. has received research funding from Chugai Pharmaceutical Co., Ltd, Bristol-Myers Squibb, Kyowa Hakko Kirin Co., Ltd, Zenyaku Kogyo Co., Ltd, FUJIFILM Corporation, Nippon Boehringer Ingelheim Co., Ltd, Astellas Pharma Inc. and Celgene Corporation, consulting fees from Astellas Pharma Inc. and Daiichi Sankyo Co., Ltd, and honoraria from Bristol-Myers Squibb, Pfizer Japan Inc. and Astellas Pharma Inc.

ORCID

Kazuyuki Shimada  <https://orcid.org/0000-0002-1075-9219>

REFERENCES

1. Swerdlow SH, Campo E, Harris NL, et al., eds. *WHO Classification of Tumours of Haematopoietic and Lymphoid Tissues*. Lyon, France: IARC Press; 2017.
2. Coiffier B, Lepage E, Briere J, et al. CHOP chemotherapy plus rituximab compared with CHOP alone in elderly patients with diffuse large-B-cell lymphoma. *N Engl J Med*. 2002;346:235-242.
3. Pfreundschuh M, Trumper L, Osterborg A, et al. CHOP-like chemotherapy plus rituximab versus CHOP-like chemotherapy alone in young patients with good-prognosis diffuse large-B-cell lymphoma: a randomised controlled trial by the MabThera International Trial (MINT) Group. *Lancet Oncol*. 2006;7:379-391.
4. Coiffier B, Thieblemont C, Van Den Neste E, et al. Long-term outcome of patients in the LNH-98.5 trial, the first randomized study comparing rituximab-CHOP to standard CHOP chemotherapy in DLBCL patients: a study by the Groupe d'Etudes des Lymphomes de l'Adulte. *Blood*. 2010;116:2040-2045.
5. Savage KJ, Johnson NA, Ben-Neriah S, et al. MYC gene rearrangements are associated with a poor prognosis in diffuse large B-cell lymphoma patients treated with R-CHOP chemotherapy. *Blood*. 2009;114:3533-3537.
6. Johnson NA, Savage KJ, Ludkovski O, et al. Lymphomas with concurrent BCL2 and MYC translocations: the critical factors associated with survival. *Blood*. 2009;114:2273-2279.
7. Barrans S, Crouch S, Smith A, et al. Rearrangement of MYC is associated with poor prognosis in patients with diffuse large B-cell lymphoma treated in the era of rituximab. *J Clin Oncol*. 2010;28:3360-3365.
8. Johnson NA, Slack GW, Savage KJ, et al. Concurrent expression of MYC and BCL2 in diffuse large B-cell lymphoma treated with rituximab plus cyclophosphamide, doxorubicin, vincristine, and prednisone. *J Clin Oncol*. 2012;30:3452-3459.
9. Ansell SM, Lesokhin AM, Borrello I, et al. PD-1 blockade with nivolumab in relapsed or refractory Hodgkin's lymphoma. *N Engl J Med*. 2015;372:311-319.

10. Armand P, Shipp MA, Ribrag V, et al. Programmed death-1 blockade with pembrolizumab in patients with classical Hodgkin lymphoma after brentuximab vedotin failure. *J Clin Oncol*. 2016;34:3733-3739.
11. Kwong YL, Chan TSY, Tan D, et al. PD1 blockade with pembrolizumab is highly effective in relapsed or refractory NK/T-cell lymphoma failing l-asparaginase. *Blood*. 2017;129:2437-2442.
12. Kalluri R. The biology and function of fibroblasts in cancer. *Nat Rev Cancer*. 2016;16:582-598.
13. Scott DW, Gascoyne RD. The tumour microenvironment in B cell lymphomas. *Nat Rev Cancer*. 2014;14:517-534.
14. Olumi AF, Grossfeld GD, Hayward SW, Carroll PR, Tlsty TD, Cunha GR. Carcinoma-associated fibroblasts direct tumor progression of initiated human prostatic epithelium. *Can Res*. 1999;59:5002-5011.
15. Shan T, Chen S, Chen X, et al. Cancer-associated fibroblasts enhance pancreatic cancer cell invasion by remodeling the metabolic conversion mechanism. *Oncol Rep*. 2017;37:1971-1979.
16. Richards KE, Zeleniak AE, Fishel ML, Littlepage LE, Hill R. Cancer-associated fibroblast exosomes regulate survival and proliferation of pancreatic cancer cells. *Oncogene*. 2016;36:1770-1778.
17. Fiaschi T, Marini A, Giannoni E, et al. Reciprocal metabolic reprogramming through lactate shuttle coordinately influences tumor-stroma interplay. *Can Res*. 2012;72:5130-5140.
18. Martinez-Outschoorn UE, Balliet RM, Rivadeneira DB, et al. Oxidative stress in cancer associated fibroblasts drives tumor-stroma co-evolution: A new paradigm for understanding tumor metabolism, the field effect and genomic instability in cancer cells. *Cell Cycle*. 2010;9:3256-3276.
19. Ye H, Adane B, Khan N, et al. Leukemic stem cells evade chemotherapy by metabolic adaptation to an adipose tissue niche. *Cell Stem Cell*. 2016;19:23-37.
20. Zhang W, Trachootham D, Liu J, et al. Stromal control of cystine metabolism promotes cancer cell survival in chronic lymphocytic leukaemia. *Nat Cell Biol*. 2012;14:276-286.
21. Sugimoto K, Hayakawa F, Shimada S, et al. Discovery of a drug targeting microenvironmental support for lymphoma cells by screening using patient-derived xenograft cells. *Sci Rep*. 2015;5:13054.
22. Aoki T, Shimada K, Sakamoto A, et al. Emetine elicits apoptosis of intractable B-cell lymphoma cells with MYC rearrangement through inhibition of glycolytic metabolism. *Oncotarget*. 2017;8:13085-13098.
23. Shimada K, Tomita A, Minami Y, et al. CML cells expressing the TEL/MDS1/EV11 fusion are resistant to imatinib-induced apoptosis through inhibition of BAD, but are resensitized with ABT-737. *Exp Hematol*. 2012;40:724-737.e2.
24. Takagi Y, Shimada K, Shimada S, et al. SPIB is a novel prognostic factor in diffuse large B-cell lymphoma that mediates apoptosis via the PI3K-AKT pathway. *Cancer Sci*. 2016;107:1270-1280.
25. Soga T, Ohashi Y, Ueno Y, Naraoka H, Tomita M, Nishioka T. Quantitative metabolome analysis using capillary electrophoresis mass spectrometry. *J Proteome Res*. 2003;2:488-494.
26. Katakai T, Hara T, Sugai M, Gonda H, Shimizu A. Lymph node fibroblastic reticular cells construct the stromal reticulum via contact with lymphocytes. *J Exp Med*. 2004;200:783-795.
27. Sakamoto A, Tsukamoto T, Furutani Y, et al. Live-cell single-molecule imaging of the cytokine receptor MPL for analysis of dynamic dimerization. *J Mol Cell Biol*. 2016;8:553-555.
28. Warburg O. On the origin of cancer cells. *Science*. 1956;123:309-314.
29. Pavlides S, Whitaker-Menezes D, Castello-Cros R, et al. The reverse Warburg effect: aerobic glycolysis in cancer associated fibroblasts and the tumor stroma. *Cell Cycle*. 2009;8:3984-4001.
30. Liberti MV, Locasale JW. The Warburg effect: how does it benefit cancer cells? *Trends Biochem Sci*. 2016;41:211-218.
31. Viale A, Pettazoni P, Lyssiotis CA, Ying H, Nature S-N. Oncogene ablation-resistant pancreatic cancer cells depend on mitochondrial function. *Nature*. 2014;514:628-632.
32. Flaveny CA, Griffett K, El-Gendy B, Cell K-M. Broad anti-tumor activity of a small molecule that selectively targets the Warburg effect and lipogenesis. *Cancer Cell*. 2015;28:42-56.

SUPPORTING INFORMATION

Additional supporting information may be found online in the Supporting Information section at the end of the article.

How to cite this article: Sakamoto A, Kunou S, Shimada K, et al. Pyruvate secreted from patient-derived cancer-associated fibroblasts supports survival of primary lymphoma cells. *Cancer Sci*. 2019;110:269-278. <https://doi.org/10.1111/cas.13873>